Title

Influence of Fe Substitution into LaCoO3 Electrocatalysts on Oxygen-Reduction Activity

Journal

ACS Applied Materials & Interfaces, 11(6)

ISSN

1944-8244

Authors

Wang, Maoyu

Han, Binghong

Deng, Junjing

et al.

Publication Date

2019-02-13

DOI

10.1021/acsami.8b20780

The Influence of Fe substitution into $LaCoO_3$-Electrocatalysts on Oxy- gen-Reduction Activity

Maoyu Wang[a†], Binghong Han[b†], Junjing Deng[c], Yi Jiang[c], Mingyue Zhou[d], Marcos Lucero[a], Yan Wang[a], Yubo Chen[e], Zhenzhen Yang[b], Alpha T N'Diaye[f], Qing Wang[d], Zhichuan J. Xu[e], and Zhenxing Feng[a*]

[a] Department of Chemical, Biological, and Environmental Engineering, Oregon State University, Corvallis, Oregon 97331,
United States

[b] Chemical Sciences and Engineering Division, Argonne National Laboratory, Argonne, Illinois 60439, United States

[c] Advanced Photon Source, Argonne National Laboratory, Argonne, Illinois 60439, United States

[d] Department of Materials Science and Engineering, Faculty of Engineering, National University of Singapore, Singapore 117576, Singapore

[e] School of Materials Science and Engineering, Nanyang Technological University, Singapore 639798, Singapore

[f] Advanced Light Source, Lawrence Berkeley National Laboratory, Berkeley, California 94720, United States

ABSTRACT: The development of commercial-friendly and stable catalysts for oxygen reduction reaction (ORR) is critical for many energy conversion systems such as fuel cells and metal-air batteries. Many Co-based perovskite oxides such as LaCoO3 have been discovered as the stable and active ORR catalysts, which can be good candidates to replace platinum (Pt). Although research- ers have tried substituting various transition metals into the Co-based perovskite catalysts to improve the ORR performance, the influence of substitution on the ORR mechanism is rarely studied. In this paper, we explore the evolution of ORR mechanism after substituting Fe into LaCoO3, using the combination of X-ray photoelectron spectroscopy, high-resolution X-ray microscopy, X-ray diffraction, surface-sensitive soft X-ray absorption spectroscopy characterization, and electrochemical tests. We observed enhanced catalytic activities and increased electron transfer numbers during the ORR in Co-rich perovskite, which are attributed to the opti- mized eg filling numbers and the stronger hybridization of transition metal 3*d* and oxygen 2*p* bands. The discoveries in this paper provide deep insights into the ORR catalysis mechanism on metal oxides and new guidelines for the design of Pt-free ORR cata- lysts.

Keywords: Oxygen Reduction Reaction, X-ray absorption spectroscopy, Electronic Structure, Perovskite, Electrocatalyst

Recent decades, the scarcity of fossil fuels and global warming drive the development in green and renewable energy resources. The energy conversion systems such as proton exchange membrane fuel cell (PEMFCs) and metal air batteries (MABs) have been considered as promising solutions.[1-3] However, the sluggish kinetics of oxygen re- duction reaction (ORR) suspends the development of PEMFCs and MABs, and the traditional platinum-based ORR catalysts account for 20% of the total cost of com- mercial PEMFCs, which hampers the commercialization of those energy conversion systems.[4] Using transition-metal oxides, particularly the perovskite oxides, to catalyze ORR in alkaline solution provides an alternative commercial- friendly solution. Recently, many experimental and compu- tational studies have been done to find the optimized per- ovskite oxides, such as $Ba0.5Sr0.5Co0.8Fe0.2O3-\delta$,4 to replace Pt-based ORR catalysts in alkaline media.[1, 5-7] Researchers have found that when the eg filling number is close to 1, the perovskite oxides tend to have higher ORR activity, which provided guidelines to improve the ORR performance of perovskite catalysts by tuning their electronic structures.[1] However, the experimental determination of eg filling

number is nontrivial. Recently, substituting transition met- als such as Fe into Co-based perovskites has been proved as an effective way to improve the ORR performance in alkaline electrolytes,[1, 4, 8] but the influence of metal substitu- tions in perovskite ORR catalysts on the evolution of elec- tronic structures and ORR mechanisms still remains un- clear.

In this work, we used Fe-substituted $LaCoO_3$ to systemati- cally study the transition metal substitution effect on the electronic structures and its consequential influence on the ORR kinetics and catalysis mechanisms. A series of $LaCo_xFe_{1-x}O_3$ ($x = 0, 0.4, 0.6, 1$) was synthesized to tune the Co 3*d* band and Co (3*d*)-O (2*p*) hybridization, which were measured by the surface-sensitive soft X-ray absorp- tion spectroscopy (XAS). We found the sluggish perfor- mance with Fe substitution can be attributed to the tuning of eg orbit electron and transition Metal-Oxygen bond (M-O) covalency. Additionally, by using the rotation-speed dependent electrochemical tests, we analyzed the change of electron transfer numbers during ORR. Fe substitution caused more two-electron-transfer reaction that reduces O_2 to H_2O_2, compared with the four-electron-transfer reaction

found on Co-rich surfaces that directly reduces O2 to H2O. The change of electron transfer number implies that the Fe substitution and the tuning of M-O covalency not only have large influence on the ORR kinetics, but also to the micro- kinetic reaction mechanisms.

The X-ray diffraction (XRD) patterns of LaCoxFe1-xO3 are shown in Figure 1. The phase transition from rhombo- hedral perovskite to orthorhombic perovskite is clearly observed with more Fe doping. The LaCoO3 and LaFeO3 have pure rhombohedral and orthorhombic structures, re- spectively, compared with the reference patterns, while the
LaCo0. $_{0.4}$O and $_{0.6}$O exhibit the mixed-phase
6Fe 3 LaCo0.4Fe 3
structures. Such phase change after substitution is con- sistent with the previous report.[9] To examine the morphol- ogy and bulk composition, we chose simultaneous X-ray [10-11]
fluorescence and ptychographic measurements, nondestructive, direct visualization with high resolution in composition and morphology, and can be applied for *in situ* measurements.[12] Figure 2 shows La, Co and Fe elemental maps of LaCoxFe1-xO3 micro-particles with a spatial resolu- tion of about 160 nm. The fluorescence results are mostly consistent with the percentage of stoichiometrically mixed La2O3, Fe2O3 and Co3O4 (see Table S3). The phase images of ptychographic reconstructions in Figure 2 show 2- dimensional projected electron density distribution of these particles with a significantly higher spatial resolution (~15 nm), which enables to reveal the internal structures within the particles. Our results suggest that all LaCoxFe1-xO3 ma- terials are synthesized in micron size with reasonable ho- mogenous elemental distribution from surface to bulk. As far as we know, this is the first X-ray ptychorgraphy imag- es for electrocatalysis applications. To quantify the surface area of LaCoxFe1-xO3, the *Brunauer–Emmett–Teller* (BET) tests were carried out and the specific surface areas of these LaCoxFe1-xO3 oxides are 0.18-0.57 m2/g, as shown in Table S2, which are consistent with the µm-scale particle size observed in X-ray images. Since the reaction takes place on the surfaces of catalysts, the X-ray photoelectron spectros- copy (XPS) was used to confirm the surface stoichiometry, which is also closely correlated with the electrochemical performance. The XPS results in Table S1 show that the surface Co: Fe ratios of different samples are consistent with their bulk nomination Co: Fe ratios.

orthorhombic structures with higher Fe substitution is observed in the zoom-in part.

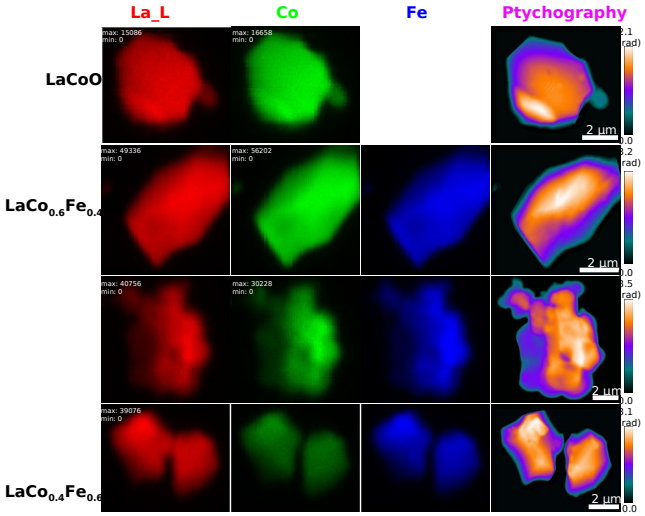

as it is

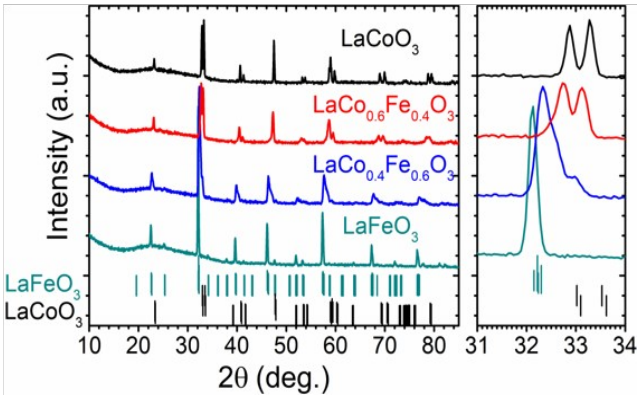

Figure 1: Powder X-ray diffraction patterns of LaCoxFe1-xO3 (x=0, 0.4, 0.6, 1). The phase transitions from rhombohedral and

Figure 2. X-ray fluorescence and ptychographic images of LaCoxFe1-xO3 (x=0, 0.4, 0.6, 1) particles to show the element dis- tribution and morphology. The La L-edge, Co K-edge and Fe K- edge fluorescence were selectively monitored to obtain corre- sponding element distribution.

The ORR performance of LaCoxFe1-xO3 was tested in 0.1M KOH solutions using the three-electrode rotating-disk method. The ORR currents of LaCoO3 measured at differ- ent rotation speeds after background correction (see Figure S1) demonstrates the transportation limit (limiting current) has critical influence particularly under high ORR overpo- tentials. With the help of electron transfer number and Equation S3, which will be discussed in detail later, we can estimate the limiting current and therefore obtain the kinet- ic current *ikinetic* using Equation S2. The kinetic ORR cur- rents density normalized by the BET surface areas of dif- ferent LaCoxFe1-xO3 are shown in Figures 3a and 3b,13 where the IR correction has been employed to correct the voltage loss from Ohmic resistance. Both the polarization curves and Tafel plots show that the increase of Fe concen- tration caused the decrease of ORR catalytic activity. The overpotential increased by 46 mV at 2 mA/cm2oxide from LaCoO3 to LaFeO3 (Figure 3a). Despite the change in ORR activity, substituting Fe into LaCoO3 did not cause obvious change in Tafel slopes, as shown in Figure 3b, demonstrat- ing that the energy barriers of the rate-determine steps on different samples are similar during the ORR.

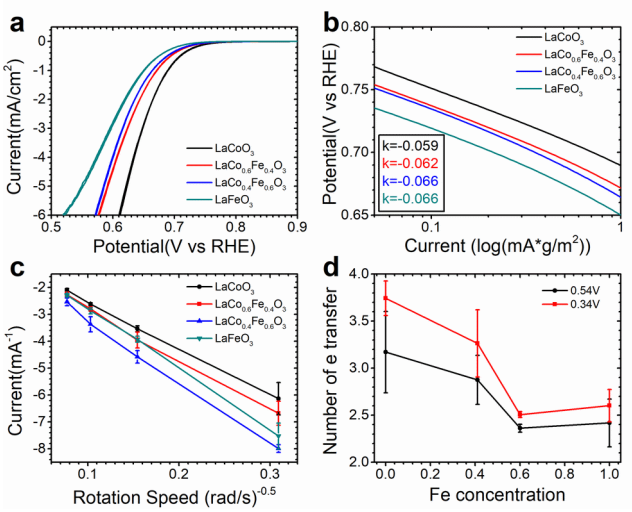

Figure 3: (a) Specific ORR activity of LaCoxFe1-xO3 (x= 0.0, 0.4, 0.6, 1) in O2-saturated 0.1M KOH solutions at the rotation rate of 1600 rpm with the scan rate of 20 mV/s, where LaCoO3 has the lowest overpotential. (b) ORR activity Tafel plots of LaCoxFe1- $_x$O3 (x= 0.0, 0.4, 0.6, 1), using the same data shown in panel a. The insert box shows the Tafel slope of each material. (c) ORR current at 0.54 V vs. RHE corrected only by background subtrac- tion as a function of rotation speeds (100, 400, 900, 1600 rpm) for the Koutecky-Levich equation. (d) Number of electron transfer determined by panel c and Figure S2 during ORR at 0.34 and 0.54 V vs. RHE against different Fe substitution levels. The number of electron transfer decreases with Fe doping. The data points repre- sent the average values from at least three measurements for each sample, while the error bars represent the corresponding standard deviations.

In addition to the Tafel slope, the electron transfer num- ber during ORR is also closely correlated with the ORR catalysis pathway. Figure 3c shows the ORR currents measured at 0.54 V vs. RHE under different rotation speeds on different samples, plotted against the inverse root of the rotation speed. Similar plot measured at 0.34 V vs. RHE is shown in Figure S2. The slope of these plots, according to the Koutecky-Levich equation, can be used to determine the number of electron transfer during ORR by comparing with that of pure Pt disk, which has 4 electron transfers for ORR catalysis. As shown in Figure 3d, from LaCoO3 to LaFeO3, the electron transfer number dropped from 3.17 to 2.42 at 0.54V vs. RHE, and dropped from 3.74 to 2.60 at 0.34 V vs. RHE. The great decrease of electron transfer number after Fe substitution indicates the Fe site prefer 2- electron-transfer ORR mechanism that reduces O2 to H2O2, while the Co site prefer 4-electron-transfer reaction that directly reduces O2 to H2O.14 Although both 2- and 4- electron-transfer pathways can reduce O2 to H2O at the end, the 2-electron-transfer pathway is not desirable for fuel cell applications since the free peroxides formed during ORR can damage the separators and the catalysts.[14] Meanwhile, the Fc/Fc+ test shown in Figure S3 indicates that the differ- ent LaCoxFe1-xO3 samples used in this paper have similarly good conductivity Therefore, the decreased electron trans- fer numbers and catalytic activities observed on Fe-rich samples are less likely due to the conductivity variation but more likely due to the electronic structure evolutions,

which can influence the bidentate and end-on O2 adsorption type on the catalyst surface and therefore affect different electron transfer pathway.[2]

In this study, we used surface-sensitive characterization techniques, including the XPS and the electron yield mode of soft XAS, to examine the oxidization state and surface electronic structures of LaCoxFe1-xO3 with different Fe sub- stitution levels. As demonstrated in our previous studies,[15-16] XAS is an element-specific technique that can provide information related to both electronic and atomic structure, and quite powerful for *in situ* characterizations. XAS measurements on the Co L-edge (Figure 4a) show an in- termediate spin state in LaCoxFe1-xO3 with eg=1, which is close to the optimized eg filling number of perovskites for ORR catalysis.[1, 17-18] In contrary, the Fe L-edge results in Figure 4b illustrates a high spin state with eg=2, which, according to previous eg descriptor studies, corresponds to much lower ORR activity.[19] Therefore, enhancing the Fe doping level will increase the average number of eg orbital electrons and diverge the electronic structure from the op- timized value around 1 (also see supporting information for details). This finding is consistent with the suppressed elec- trochemical performance after Fe substitution observed in Figure 3a. In addition, a small peak around 783 eV can be observed in the Co L-edge of LaCo0.4Fe0.6O3 (see Figure 4a), indicating that when the Fe substitution level is too high, the surface Co trends to partially assume the low spin state, which also increases the average eg filling number.18 Here the change of eg filling number can explain the slower ORR kinetics after substituting Co with Fe. However, no previous eg orbital theory can be used to explain the differ- ent reaction pathways with different electron transfer num- bers observed on various LaCoxFe1-xO3 samples in Figure 3d. Actually, most of the previous mechanism studies on the ORR electron transfer numbers focused on the oxygen species adsorbed on the catalyst surface during ORR. One study proposed that the nature of the adsorption of oxygen species on metal oxides, which is related to the interaction between oxygen π orbitals and metal d ^{2} orbitals, could be different between Fe-based oxides and Co-based oxides, since Fe has filled d ^{2} (Pauling model) while Co has empty dz2 (Griffths or Bridge model).8 The difference of oxygen- metal interactions on the surface may influence the final electron transfer number during ORR. In addition to oxy- gen-metal interactions, the surface oxidization status of transition metal sites may also be a descriptor for the ORR performance and electron transfer numbers. By comparing with Fe and Co XPS (Figure S5), we observed no change in Co and Fe oxidization states after Fe doping, meaning Fe substitution will not influence the oxidization states of Co and Fe on the surface, implying a weak interaction between Co and Fe. Therefore, Co prefers the 4-eletron pathway, and Fe prefers the 2-electron pathway.

z

z

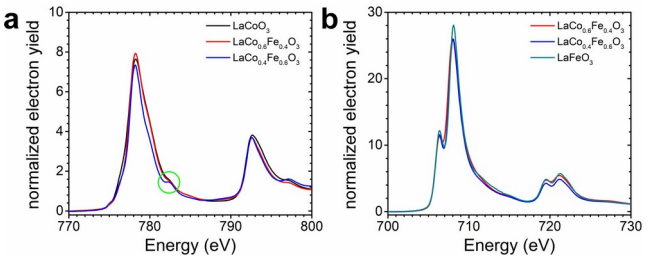

Figure 4: Surface-sensitive soft XAS electron yield mode data of
(a) Co L-edge and (b) Fe L-edge represents the change of transi- tion metal 3d spin state after the Fe substitution into LaCoO3.

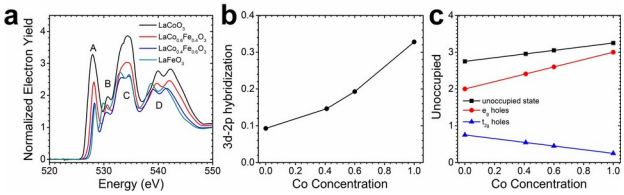

Figure 5: (a) O K-edge spectroscopy in surface-sensitive yield mode of LaCoxFe1-xO3 (x= 0.0, 0.4, 0.6, 1). Peak A represents the Fe/Co 3d and O 2p hybridized states correlated with ORR catalyt- ic activity. (b) Estimated 3d-2p hybridization by integration the peak A area as a function of surface Co ratio. (c) Calculated amount of eg holes, t2g holes and unoccupied states related corre- lated with surface Co-ratio by using high spin Fe(III) and inter- mediate spin Co (III).

In addition to the investigation of metal oxidation states using metal L-edge results to explain the change of electron transfer numbers on different metal sites, we further ap- plied XAS (Figure 5) and XPS (Figure S4) on the oxygen K-edge to quantify the role of M-O covalency in ORR mechanisms. Figure 5 shows the oxygen K-edge XAS re- sults on different samples, where peak A is the covalent or hybridization mixing of oxygen 2*p* state with transition metal 3*d* state, peak B is due to the oxygen octahedral co- ordination, peak C is the mixed states of oxygen 2*p* state and lanthanum 5*d* state, and peak D is the mixed state of transition metal 4*sp* and lanthanum 5*sp*.[20-22] In a previous in-situ O K-edge XAS study, when different potentials were applied on the oxide catalysts, only peak A showed clear changes, which indicates peak A (i.e. the M-O cova- lency) is the most important property that is related to the oxygen adsorption and redox processes.[5] By calculating the area of peak A,[1] we can estimate the M-O hybridization of different perovskites, as shown in Figure 5b, which implies the reducing of M-O hybridization with increasing Fe con- tents. Previous studies on perovskite oxide for oxygen evo- lution reaction (OER) catalysis showed that a stronger M-O hybridization can optimize the oxygen adsorption, activate oxygen redox, and therefore reduce the overpotential re- quired for 4-step OER process on perovskite oxides.[9, 23] However, few studies have been focused on the influence of M-O hybridization on the ORR catalysis. In this study, we showed that the increase of M-O covalency with less Fe and more Co in the perovskite B site can also accelerate the ORR kinetics, probably still due to the optimization of sur- face oxygen adsorption and the activation of oxygen redox observed for OER process. Furthermore, according to Fig-

ure 3d, a stronger hybridization between oxygen 2*p* band and metal 3*d* band in Co-rich samples also leads to a more beneficial 4-electron-transfer ORR pathway, which might be due to the reduction of the required overpotentials for the 4-step ORR mechanism. The intensity of peak A is also assigned to unoccupied states of Fe/Co 3*d*-O2*p* states gen- erated by the Fe/Co 3*d* and O2*p* hybridization and linearly proportional to the total number of the empty Fe/Co 3*d*- O2*p* state.[5, 24] The surface oxidization state of Co and Fe can be roughly estimated by analyzing peak positions and peak shapes of XAS (Figure 4) and XPS (Figure S5) result. Comparing with XAS and XPS results in previous litera- ture, we find the surface Co and Fe are roughly Co(III) and Fe(III).25-28 Then the amount of eg holes, t2g holes and unoc- cupied states have been calculated in Figure 5c using the intermediate spin Co(III) and high spin Fe(III).[1, 24] Figures 5a and 5c indicate less unoccupied states with more Fe doping. Since it is the highest unoccupied electronic ex- changes electrons with the oxygen adsorbate species, more electrons in the highest unoccupied states (eg) after Fe dop- ing lead to stronger electron exchange with the adsorbed oxygen species, which can facilitate the releasing of free peroxides and promote the 2-electron transfer pathway dur- ing the ORR.[5] This conclusion emphasizes that the elec- tronic structure determines the reaction pathway, and is supported by previous study which found Fe(IV) can pro- mote 4-electron-transfer (Note Fe(IV) has the same eg elec- tron as Co(III), but different from Fe(III) with eg=2).29

In summary, we have studied the role of Fe substitution to tune the catalytic performance and ORR reaction mech- anism. We observed the reduced catalysis activity and the decrease electron transfer number during the ORR process on perovskites with more Fe substitution. The sluggish ORR kinetics and less preferable 2-electron-transfer path- way observed in Fe-substituted perovskites is attributed to the increase of eg filling number and decrease of M-O co-valency observed in the soft XAS results. This paper pro- vides deep insights to the effect of electronic structures on the ORR kinetics and mechanisms, as well as guidelines to develop more active oxide catalysts with preferred ORR pathway in the future.

ASSOCIATED CONTENT

Supporting Information

This material is available free of charge via the Internet at http://pubs.acs.org.

Electrochemical performance, Conductivity measure- ments, X-ray photoelectron spectroscopy characterization, X-ray fluorescence spectrum

AUTHOR INFORMATION

† These authors contributed equally to this work

*Corresponding author:

E-mail: zhenxing.feng@oregonstate.edu

ACKNOWLEDGMENT

This work was financially supported by Callahan Faculty Scholar Endowment and start-up funds from Oregon State University. The

hard X-ray microscopy measurements were done at 2-ID-D of Advanced Photon Source, which is a U.S. Department of Energy (DOE) Office of Science User Facility operated for the DOE Of- fice of Science by Argonne National Laboratory under Contract No. DE-AC02-06CH11357. The soft X-ray absorption spectros- copy was performed at beamline 6.3.1 of Advanced Light Source, which is an Office of Science User Facility operated for the U.S. DOE Office of Science by Lawrence Berkeley National Laborato- ry and supported by the DOE under Contract No. DEAC02- 05CH11231. Authors thank Anton Paar USA, Inc. for the BET tests.

REFERENCE

(1) Suntivich, J.; Gasteiger, H. A.; Yabuuchi, N.; Nakanishi, H.; Goodenough, J. B.; Shao-Horn, Y. Design Principles for Oxygen- Reduction Activity on Perovskite Oxide Catalysts for Fuel Cells and Metal-Air Batteries. *Nat Chem* **2011,** *3*, 647-647, DOI: 10.1038/Nchem.1093.

(2) Wang, Z. L.; Xu, D.; Xu, J. J.; Zhang, X. B. Oxygen Electrocata- lysts in Metal-air Batteries: from Aqueous to Nonaqueous Electro- lytes. *Chem Soc Rev* **2014,** *43*, 7746-7786, DOI: 10.1039/c3cs60248f.

(3) Li, H. Y.; Sun, S. N.; Xi, S. B.; Chen, Y. B.; Wang, T.; Du, Y. H.; Sherburne, M.; Ager, J. W.; Fisher, A. C.; Xu, Z. C. J. Metal-Oxygen Hybridization Determined Activity in Spinel-Based Oxygen Evolu- tion Catalysts: A Case Study of ZnFe2-xCrxO4. *Chemistry of Materi- als* **2018,** *30*, 6839-6848, DOI: 10.1021/acs.chemmater.8b02871.

(4) Fabbri, E.; Mohamed, R.; Levecque, P.; Conrad, O.; Kotz, R.; Schmidt, T. J. Composite Electrode Boosts the Activity of Ba0.5Sr0.5Co0.8Fe0.2O3-delta Perovskite and Carbon toward Oxy- gen Reduction in Alkaline Media. *Acs Catalysis* **2014,** *4*, 1061-1070, DOI: 10.1021/cs400903k.

(5) Mueller, D. N.; Machala, M. L.; Bluhm, H.; Chueh, W. C. Redox Activity of Surface Oxygen Anions in Oxygen-deficient Perovskite Oxides during Electrochemical Reactions. *Nature Communications* **2015,** *6*, DOI: 10.1038/ncomms7097.

(6) Hwang, J.; Rao, R. R.; Giordano, L.; Katayama, Y.; Yu, Y.; Shao- Horn, Y. Perovskites in catalysis and electrocatalysis. *Science* **2017,** *358*, 751-756, DOI: 10.1126/science.aam7092.

(7) Cho, S. A.; Jang, Y. J.; Lim, H. D.; Lee, J. E.; Jang, Y. H.; Ngu- yen, T. T. H.; Mota, F. M.; Fenning, D. P.; Kang, K.; Shao-Horn, Y.; Kim, D. H. Hierarchical Porous Carbonized Co3O4 Inverse Opals via Combined Block Copolymer and Colloid Templating as Bifunctional Electrocatalysts in Li-O-2 Battery. *Adv Energy Mater* **2017,** *7*, DOI: 10.1002/aenm.201700391.

(8) Cheriti, M.; Kahoul, A. Double Perovskite Oxides Sr2MMoO6 (M
= Fe and Co) as Cathode Materials for Oxygen Reduction in Alkaline Medium. *Mater Res Bull* **2012,** *47*, 135-141, DOI: 10.1016/j.materresbull.2011.09.016.

(9) Duan, Y.; Sun, S. N.; Xi, S. B.; Ren, X.; Zhou, Y.; Zhang, G. L.; Yang, H. T.; Du, Y. H.; Xu, Z. C. J. Tailoring the Co 3d-O 2p Cova- lency in LaCoO3 by Fe Substitution to Promote Oxygen Evolution Reaction. *Chemistry of Materials* **2017,** *29*, 10534-10541, DOI: 10.1021/acs.chemmater.7b04534.

(10) Deng, J.; Lo, Y. H.; Gallagher-Jones, M.; Chen, S.; Pryor, A.; Jin, Q.; Hong, Y. P.; Nashed, Y. S. G.; Vogt, S.; Miao, J.; Jacobsen,
C. Correlative 3D x-ray Fluorescence and Ptychographic Tomography of Frozen-hydrated Green Algae. *Science Advances* **2018,** *4*, DOI: 10.1126/sciadv.aau4548.

(11) Deng, J. J.; Vine, D. J.; Chen, S.; Nashed, Y. S. G.; Jin, Q. L.; Phillips, N. W.; Peterka, T.; Rossc, R.; Vogt, S.; Jacobsen, C. J. Sim- ultaneous Cryo X-ray Ptychographic and Fluorescence Microscopy of Green Algae. *P Natl Acad Sci USA* **2015,** *112*, 2314-2319, DOI: 10.1073/pnas.1413003112.

(12) Pfeiffer, F. X-ray Ptychography. *Nat Photonics* **2018,** *12*, 9-17, DOI: 10.1038/s41566-017-0072-5.

(13) Sun, S. N.; Li, H. Y.; Xu, Z. C. J. Impact of Surface Area in Evaluation of Catalyst Activity. *Joule* **2018,** *2*, 1024-1027, DOI: 10.1016/j.joule.2018.05.003.

(14) Wroblowa, H. S.; Pan, Y. C.; Razumney, G. Electroreduction of Oxygen - New Mechanistic Criterion. *J Electroanal Chem* **1976,** *69*, 195-201, DOI: Doi 10.1016/S0022-0728(76)80250-1.
(15) Weng, Z.; Wu, Y. S.; Wang, M. Y.; Jiang, J. B.; Yang, K.; Huo,
S. J.; Wang, X. F.; Ma, Q.; Brudvig, G. W.; Batista, V. S.; Liang, Y. Y.; Feng, Z. X.; Wang, H. L. Active Sites of Copper-complex Cata- lytic Materials for Electrochemical Carbon Dioxide Reduction. *Na- ture Communications* **2018,** *9*, 415, DOI: 10.1038/s41467-018-02819- 7.
(16) Cai, Z.; Zhou, D. J.; Wang, M. Y.; Bak, S. M.; Wu, Y. S.; Wu, Z. S.; Tian, Y.; Xiong, X. Y.; Li, Y. P.; Liu, W.; Siahrostami, S.; Kuang, Y.; Yang, X. Q.; Duan, H. H.; Feng, Z. X.; Wang, H. L.; Sun, X. M. Introducing Fe2+ into Nickel-Iron Layered Double Hydroxide: Local Structure Modulated Water Oxidation Activity. *Angew Chem Int Edit* **2018,** *57*, 9392-9396, DOI: 10.1002/anie.201804881.
(17)Haverkort, M. W.; Hu, Z.; Cezar, J. C.; Burnus, T.; Hartmann, H.; Reuther, M.; Zobel, C.; Lorenz, T.; Tanaka, A.; Brookes, N. B.; Hsieh, H. H.; Lin, H. J.; Chen, C. T.; Tjeng, L. H. Spin State Transi- tion in LaCoO3 Studied Using Soft X-ray Absorption Spectroscopy and Magnetic Circular Dichroism. *Phys Rev Lett* **2006,** *97*, 176405, DOI: 10.1103/PhysRevLett.97.176405.
(18) Kumagai, Y.; Ikeno, H.; Oba, F.; Matsunaga, K.; Tanaka, I. Ef- fects of Crystal Structure on Co-L(2,3) X-ray Absorption Near-edge Structure and Electron-energy-loss Near-edge Structure of Trivalent Cobalt Oxides. *Phys Rev B* **2008,** *77*, 155124, DOI: 10.1103/PhysRevB.77.155124.
(19)Hocking, R. K.; George, S. D.; Raymond, K. N.; Hodgson, K. O.; Hedman, B.; Solomon, E. I. Fe L-Edge X-ray Absorption Spec- troscopy Determination of Differential Orbital Covalency of Sidero- phore Model Compounds: Electronic Structure Contributions to High Stability Constants. *J Am Chem Soc* **2010,** *132*, 4006-4015, DOI: 10.1021/ja9090098.
(20) Anjum, G.; Kumar, R.; Mollah, S.; Thakur, P.; Gautam, S.; Chae,
K. H. NEXAFS Studies of La(0.8B)i(0.2)Fe(1-x)Mn(x)O(3) (0.0 <= x
<= 0.4) Multiferroic System Using X-ray Absorption Spectroscopy. *J Phys D Appl Phys* **2011,** *44*, 075403, DOI: 10.1088/0022- 3727/44/7/075403.
(21) Toulemonde, O.; N'Guyen, N.; Studer, F.; Traverse, A. Spin State Transition in LaCoO3 with Temperature or Strontium Doping as Seen by XAS. *J Solid State Chem* **2001,** *158*, 208-217, DOI: DOI 10.1006/jssc.2001.9094.
(22) Lafuerza, S.; Subias, G.; Garcia, J.; Di Matteo, S.; Blasco, J.; Cuartero, V.; Natoli, C. R. Origin of the Pre-peak Features in the Xxygen K-edge X-ray Absorption Spectra of LaFeO3 and LaMnO3 Studied by Ga Substitution of the Transition Metal Ion. *J Phys-Condens Mat* **2011,** *23*, 325601, DOI: 10.1088/0953-8984/23/32/325601.
(23) Grimaud, A.; Demortière, A.; Saubanère, M.; Dachraoui, W.; Duchamp, M.; Doublet, M.-L.; Tarascon, J.-M. Activation of Surface Oxygen Sites on an Iridium-based Model Catalyst for the Oxygen Evolution Reaction. **2016,** *2*, 16189, DOI: 10.1038/nenergy.2016.189.
(24) Suntivich, J.; Hong, W. T.; Lee, Y. L.; Rondinelli, J. M.; Yang,
W. L.; Goodenough, J. B.; Dabrowski, B.; Freeland, J. W.; Shao- Horn, Y. Estimating Hybridization of Transition Metal and Oxygen States in Perovskites, from O K-edge X-ray Absorption Spectroscopy. *J Phys Chem C* **2014,** *118*, 1856-1863, DOI: 10.1021/jp410644j.
(25)Mcintyre, N. S.; Zetaruk, D. G. X-Ray Photoelectron Spectro- scopic Studies of Iron-Oxides. *Anal Chem* **1977,** *49*, 1521-1529, DOI: DOI 10.1021/ac50019a016.
(26)Wang, K. X.; Niu, H. L.; Chen, J. S.; Song, J. M.; Mao, C. J.; Zhang, S. Y.; Zheng, S. J.; Liu, B. Z.; Chen, C. L. Facile Synthesis of CeO2-LaFeO3 Perovskite Composite and Its Application for 4- (Methylnitrosamino)-1-(3-Pyridyl)-1-Butanone (NNK) Degradation. *Materials* **2016,** *9*, 326, DOI: 10.3390/ma9050326.
(27) Wasinger, E. C.; de Groot, F. M. F.; Hedman, B.; Hodgson, K. O.; Solomon, E. I. L-edge X-ray Absorption Spectroscopy of Non- heme Iron Sites: Experimental Determination of Differential Orbital Covalency. *J Am Chem Soc* **2003,** *125*, 12894-12906, DOI: 10.1021/ja034634s.

(28) Miedema, P. S.; de Groot, F. M. F. The Iron L edges: Fe 2p X- ray Absorption and Electron Energy Loss Spectroscopy. *J Electron Spectrosc* **2013,** *187*, 32-48, DOI: 10.1016/j.elspec.2013.03.005.
(29) Zhu, Y. L.; Zhou, W.; Yu, J.; Chen, Y. B.; Liu, M. L.; Shao, Z. P. Enhancing Electrocatalytic Activity of Perovskite Oxides by Tun- ing Cation Deficiency for Oxygen Reduction and Evolution Reac- tions. *Chemistry of Materials* **2016,** *28* (6), 1691-1697, DOI: 10.1021/acs.chemmater.5b04457.

TABLE OF CONTENT